

# Critical behavior of the contact process in annealed scale-free networks

Jae Dong Noh

*Department of Physics, University of Seoul, Seoul 130-743, Korea*

Hyunggyu Park

*School of Physics, Korea Institute for Advanced Study, Seoul 130-722, Korea*

(Received 25 November 2008; published 29 May 2009)

The critical behavior of the contact process is studied in annealed scale-free networks by mapping it on the random-walk problem. We obtain the analytic results for the critical scaling using the event-driven dynamics approach. These results are confirmed by numerical simulations. The disorder fluctuation induced by the sampling disorder in annealed networks is also explored. Finally, we discuss over a possible discrepancy of the finite-size-scaling theory in annealed and quenched networks in spirit of the droplet size scale and the linking disorder fluctuation.

DOI: 10.1103/PhysRevE.79.056115

PACS number(s): 89.75.Hc, 05.40.-a, 64.60.Ht

## I. INTRODUCTION

Critical phenomena in complex networks have been attracting a lot of interest [1]. Complex networks are characterized by a so-called small-world property [2]. The number of neighbors of a node increases exponentially with the distance from it. For this property, it is believed that critical phenomena in complex networks belong to the mean-field universality class. Nevertheless, structural heterogeneity leads to rich behaviors. For example, in scale-free (SF) networks having a power-law degree distribution  $P(k) \sim k^{-\gamma}$  [3], mean-field critical exponents may vary with the degree exponent  $\gamma$  [1].

Recent studies raise an important issue on the finite-size-scaling (FSS) theory in complex networks [4,5]. A scale-free network with  $N$  nodes has a maximum cutoff  $k_{\max}$  in degree. In most cases without any constraint, the cutoff scales as  $k_{\max} \sim N^{1/(\gamma-1)}$ , which is determined by the condition  $\sum_{k>k_{\max}} P(k) = 1/N$ . This is called the natural cutoff. One may impose a forced cutoff

$$k_{\max} = N^{1/\omega} \quad (1)$$

with the cutoff exponent  $\omega > \gamma - 1$ . Taking the thermodynamic limit, one should take the limit  $N \rightarrow \infty$  and  $k_{\max} \rightarrow \infty$  simultaneously. This may give rise to an intricate finite-size effect [5].

Hong *et al.* [4] developed a FSS theory based on the single-parameter scaling hypothesis. Their theory predicts the values of the FSS exponents in the Ising model (including a more general equilibrium  $\phi^n$  theory) and the contact process (CP), respectively. The CP is a reaction-diffusion model describing an epidemic spreading, which exhibits a prototype nonequilibrium phase transition from an inactive phase into an active phase [6]. It has been suggested that the FSS exponents depend only on the degree exponent  $\gamma$ , regardless of the cutoff if it is not strong enough ( $\omega < \gamma$ ). Note that this condition includes networks with the natural cutoff ( $\omega = \gamma - 1$ ) as well as networks with a weak forced cutoff ( $\gamma - 1 < \omega < \gamma$ ). These results were confirmed numerically in the static model [7] having the natural cutoff and the uncorrelated configuration model (UCM) [8].

Castellano and Pastor-Satorras [5] considered the CP in the so-called random neighbor (annealed) network. Links are not fixed but fluctuate in this annealed network. At each time step, the neighbors of a node are chosen independently and randomly according to the degree distribution. It contrasts with a network where links are fixed permanently in time once they are formed. In order to stress the distinction, the former network will be referred to as an *annealed* network, while the latter network as a *quenched* network. From the analysis of the survival probability at the critical point, they found that the dynamic exponent characterizing the relaxation time depends not only on  $\gamma$  but also on  $\omega$  when  $\omega > \gamma - 1$  (all networks with a forced cutoff) and  $2 < \gamma < 3$ . In particular, it has been shown that there are two different characteristic time (and also the order parameter) scales which make a single-parameter scaling impossible. From the relaxation-time scaling, the order parameter in the quasi-steady-state also scales with  $N$  with an exponent depending on both  $\gamma$  and  $\omega$ .

At a glance, the results of Refs. [4,5] seem incompatible (single-parameter versus two-parameter scaling and cutoff-independent versus cutoff-dependent scaling) when  $\gamma - 1 < \omega < \gamma$  (weak forced cutoff) and  $2 < \gamma < 3$  (highly heterogeneous regime). But it is not true. The FSS theory of Ref. [4] concerns a quenched scale-free network, while that of Ref. [5] concerns an annealed scale-free network. Quenched disorder in linking topology generates local correlations through quenched links between nodes, which are responsible for the shift of the phase-transition point and its disorder fluctuations. Therefore, one may not rule out a possibility that the disorder fluctuations near the phase-transition point may wipe away or at least significantly alter the cutoff-dependent scaling regime, see Sec. VI.

In this paper, we present a full FSS theory governing the critical and off-critical scaling behaviors of the CP in annealed networks. In Sec. II, an annealed network is introduced without any sampling disorder and the heterogeneous mean-field theory is briefly reviewed for the CP. The critical dynamics is analyzed in Sec. III, while the off-critical scaling is investigated in Sec. IV. In Sec. V, we discuss the effect of sampling disorder in annealed networks and its self-averaging property. Finally, we summarize our results along

with a brief discussion on the effect of linking disorder in quenched networks.

## II. CP IN ANNEALED NETWORKS

We consider the annealed scale-free networks with the degree distribution  $P(k)=ak^{-\gamma}$  for  $k_{\min}\leq k\leq k_{\max}$  with a normalization constant  $a$  and  $P(k)=0$  elsewhere. The maximum degree  $k_{\max}$  scales with network size  $N$  as in Eq. (1) and the minimum degree  $k_{\min}$  is an  $O(1)$  constant. Since neighbors of each node need not be specified, an annealed network is realized by choosing a degree sequence  $\{k_1, \dots, k_N\}$  only.

There are two different ways in choosing the degree sequence. One may assign degree  $k$  to  $N_k$  nodes deterministically in such a way that  $\sum_{k'\geq k}N_{k'}=\text{int}[N\sum_{k'\geq k}P(k')]$  for all  $k$  in the decreasing order starting from  $k_{\max}$ , where  $\text{int}[x]$  is the integer part of  $x$ . One may easily show that the maximum degree realized using this assignment algorithm is the same order in  $N$  of a given  $k_{\max}$  when  $\omega\geq\gamma-1$ . Or one may draw probabilistically  $N$  values of  $k$  in accordance with the probability distribution  $P(k)$ . The probabilistic method yields an ensemble of different samples, which makes an ensemble average necessary. We mainly consider the annealed network realized by the deterministic method. Sample-to-sample fluctuations in the ensemble generated by the probabilistic method will be discussed in Sec. V.

The CP on the annealed SF network is defined as follows. Each node is either occupied by a particle or empty. A particle on a node is annihilated with probability  $p$  or branches one offspring to its *neighbor*, if empty, with probability  $(1-p)$ . At each time step, a neighbor of a node is selected among all the other nodes with probabilities proportional to their degree. Since a node is coupled only probabilistically with all the other nodes, the mean-field theory becomes exact in the annealed network.

Let  $n(t)$  be the number of particles at time  $t$ . Following Ref. [5] in a quasistatic approximation for large  $t$ , it increases by 1 with probability

$$w_+=p\lambda\rho\sum_k\frac{kP(k)}{\langle k\rangle}\frac{1}{1+\lambda\rho k/\langle k\rangle} \quad (2)$$

or decreases by 1 with probability

$$w_-=p\rho \quad (3)$$

after a time step  $\Delta t=1/N$ . Here  $\rho=n/N$  is the particle density and  $\lambda=(1-p)/p$  with the mean degree  $\langle k\rangle$ .

The transition probability  $w_+$  contains a nontrivial  $\rho$  dependence. When the thermodynamic limit is taken first [4] or the density is high ( $\rho\gg 1/k_{\max}$ ) in finite networks [5], one may arrive at a singular expansion

$$w_+/p=\lambda\rho-c\rho^{\theta-1}+\cdots, \quad (4)$$

with a constant  $c$  and

$$\theta=\min\{\gamma,3\}. \quad (5)$$

When the density is low ( $\rho\ll 1/k_{\max}$ ) in finite networks, one can expand the denominator in Eq. (2) to obtain

$$w_+/p=\lambda\rho-\lambda^2g\rho^2+\cdots, \quad (6)$$

where  $g=\langle k^2\rangle/\langle k\rangle^2$  with  $\langle k^n\rangle\equiv\sum_kk^nP(k)$ . Note that  $g$  is an  $O(1)$  constant for  $\gamma>3$ , while it scales as  $g\sim k_{\max}^{3-\gamma}\sim N^{(3-\gamma)/\omega}$  for  $2<\gamma<3$ . The scaling behavior can be rewritten as

$$g\sim k_{\max}^{3-\theta}\sim N^{(3-\theta)/\omega} \quad (7)$$

for general  $\gamma(\neq 3)$  and  $\omega\geq\gamma-1$ . At  $\gamma=3$ ,  $g\sim\log N$ .

As the stochastic fluctuation  $(\Delta\rho)/\rho$  (multiplicative diffusive noise) becomes negligible in the  $N\rightarrow\infty$  limit, one can write the rate equation for the average particle density in the continuum limit as

$$\frac{dp}{dt}=w_+-w_-. \quad (8)$$

It is clear that the system undergoes an absorbing phase transition at  $p=p_c=1/2(\lambda_c=1)$  at all values of  $\gamma>2$  in the thermodynamic limit. The particle density near the critical point scales as  $\rho\sim(\lambda-\lambda_c)^\beta$  with the order-parameter exponent  $\beta=1/(\theta-2)$  [4]. At  $\gamma=3$ , an additional logarithmic correction appears as  $\rho\sim(\lambda-\lambda_c)/|\log(\lambda-\lambda_c)|$ .

## III. CRITICAL DYNAMICS

We consider the CP at the critical point ( $p=1/2$  or  $\lambda=1$ ). One may regard the particle number  $n$  ( $0\leq n\leq N$ ) as a coordinate of a one-dimensional random walker [5]. At each time step  $\Delta t=1/N$ , the walker jumps to the right with probability  $w_+$  or to the left with probability  $w_-$ , or does not move with probability  $1-(w_++w_-)$ . The walker is bounded by an absorbing wall at  $n=0$  and a reflecting wall at  $n=N$ . Reaching the absorbing wall, it will be trapped there forever.

It turns out that an event-driven dynamics is useful. In this dynamics, the walker always makes a jump at each time step  $\Delta\tau=1$  to the right or left with probabilities

$$\tilde{w}_\pm=\frac{w_\pm}{w_++w_-}. \quad (9)$$

This is equivalent to the original problem if one rescales the time with the relation

$$dt=\frac{1}{N}\frac{d\tau}{w_++w_-}. \quad (10)$$

### A. Defect dynamics

It is interesting to study how particles spread starting from a localized seed. Dynamics initiated from a single particle is called the defect dynamics [6,9]. So its initial condition is  $n(0)=n_0=1$ .

Quantities of interest are the survival probability  $P_s(t)$ , the probability that the system is still active at time  $t$ , and  $n_s(t)$ , the number of particles averaged over surviving samples. At the critical point, they exhibit the power-law scalings

$$P_s(t)\sim t^{-\delta} \quad \text{and} \quad n_s(t)\sim t^{\tilde{\eta}} \quad (11)$$

for  $t < t_c(N)$  with the relaxation-time scaling as

$$t_c \sim N^{\bar{z}}. \quad (12)$$

At  $t=t_c$ , the system starts to feel its finite size and  $n_s(t)$  saturates. For  $t > t_c$ ,  $P_s(t)$  decays exponentially. The critical exponents  $\delta$ ,  $\tilde{\eta}$ , and  $\bar{z}$  are universal. Note that  $\tilde{\eta} = \delta + \eta$  where  $\eta$  is the particle number growing exponent for all samples.

Initially,  $\rho_0 = n_0/N$  is so small (much smaller than  $1/k_{\max}$ ) that one can always use the expansion in Eq. (6) for  $w_+$ . We will confirm that this is valid throughout the defect dynamics. Then, in the event-driven dynamics, the jumping probability for the walker at site  $n$  is given by

$$\tilde{w}_+ = \frac{1-g\rho}{2-g\rho} \quad \text{and} \quad \tilde{w}_- = \frac{1}{2-g\rho}$$

for small  $\rho$ . This shows that the walker performs biased walks toward the absorbing wall with the drift velocity

$$v_{drift} \equiv \frac{dn}{d\tau} = \tilde{w}_+ - \tilde{w}_- = -\frac{g\rho}{2-g\rho}. \quad (13)$$

The bias is negligible ( $v_{drift}/\tilde{w}_{\pm} \ll 1$ ) during the initial stage since  $g\rho \ll 1$ . Hence, for sufficiently small  $\tau$ , it suffices to consider the unbiased random-walk motion in the presence of the absorbing wall at  $n=0$ . The effect of the absorbing wall can be taken into account by using the image method [10]. This yields that the surviving probability decays as

$$P_s(\tau) \simeq n_0(\pi\tau/2)^{-1/2} \quad (14)$$

and that the surviving walker spreads out diffusively as

$$n_s(\tau) \simeq \sqrt{\pi\tau/2}. \quad (15)$$

The diffusion velocity for the surviving walkers is given by

$$v_{diffuse} \equiv n_s(\tau)/\tau \simeq \sqrt{\pi/(2\tau)} \simeq \pi/(2n_s). \quad (16)$$

As  $\tau$  increases, the diffusion velocity becomes smaller while the bias becomes stronger. The walker reaches a stationary state when the diffusion velocity and the drift velocity are balanced. The condition  $v_{diffuse} \sim |v_{drift}|$  yields that the walker reaches the stationary state at position

$$n_s^{\infty} \sim \sqrt{N/g}, \quad (17)$$

and at time

$$\tau_c \sim N/g. \quad (18)$$

This result is self-consistent with the underlying assumptions that  $\rho k_{\max} \ll 1$  and  $g\rho \ll 1$ .

The time scales  $t$  and  $\tau$  are related through Eq. (10). Using Eqs. (10) and (15), one finds that

$$t \simeq \int^{\tau} \frac{d\tau'}{n(\tau')} \sim \sqrt{\tau}. \quad (19)$$

Therefore we conclude that

$$P_s(t) \sim n_0 t^{-1}, \quad (20)$$

$$n_s(t) \sim t, \quad (21)$$

$$t_c \sim \sqrt{N/g}, \quad (22)$$

which leads to

$$\delta = 1, \quad (23)$$

$$\tilde{\eta} = 1 \quad (\eta = 0), \quad (24)$$

$$\bar{z} = (1 - (3 - \theta)/\omega)/2. \quad (25)$$

The result for  $\delta$  and  $\bar{z}$  coincides with that of Ref. [5]. At  $\gamma = 3$ ,  $t_c \sim n_s^{\infty} \sim (N/\log N)^{1/2}$ .

## B. Static dynamics

The static dynamics starts with the initial condition that all nodes are occupied,  $n_0 = N$  ( $\rho_0 = 1$ ). We consider the scaling behavior of  $\rho_s$ , the particle density averaged over the surviving samples.

The rate Eq. (8) takes a different form depending on the particle density. When  $\rho k_{\max} \gg 1$ , it becomes  $d\rho/dt = -c\rho^{\theta-1}/2$ , which yields

$$\rho_s(t) \sim t^{-1/(\theta-2)}. \quad (26)$$

If the density becomes sufficiently small such that  $\rho k_{\max} \ll 1$ , then the rate equation should be replaced by  $d\rho/dt = -g\rho^2/2$ , which yields the solution

$$\rho_s(t) \sim (gt)^{-1}. \quad (27)$$

The crossover between the two regimes takes place at time

$$t_* \sim g^{(\theta-2)/(3-\theta)} \sim N^{\bar{z}_*} \quad \text{with} \quad \bar{z}_* = (\theta-2)/\omega. \quad (28)$$

At this crossover time scale  $t = t_*$ , the system starts to feel the finite upper bound of the maximum degree,  $k_{\max}$ . The density at the crossover is given by

$$\rho_* \sim g^{-1/(3-\theta)} \sim N^{-\alpha_*} \quad \text{with} \quad \alpha_* = 1/\omega. \quad (29)$$

Finally, the system reaches the stationary state. From Eq. (17), the particle density at the stationary state is given by

$$\rho_s^{\infty} \sim \sqrt{1/(gN)} \sim N^{-\alpha} \quad \text{with} \quad \alpha = (1 + (3 - \theta)/\omega)/2. \quad (30)$$

The saturation time  $t_c$  determined from  $(gt_c)^{-1} \sim N^{-\alpha}$  has the same scaling behavior as the relaxation time in the defect dynamics [see Eqs. (22) and (25)]. This means that the finite systems reach the stationary state at the same time scale, irrespective of the initial conditions.

There are a few remarks. For  $\omega > \gamma - 1$  and  $\gamma < 3(\theta = \gamma)$ , there exist two distinct  $N$ -dependent time scales  $t_* \sim N^{\bar{z}_*}$  and  $t_c \sim N^{\bar{z}}$  with  $\bar{z}_* < \bar{z}$ . The former comes into play due to the finiteness of the maximum degree  $k_{\max} \sim N^{1/\omega}$ , while the latter is the time scale to reach the stationary state in finite networks. This implies that the finite-size effects in the annealed SF networks depend on the limiting procedure of how  $N$  and  $k_{\max}$  are taken to infinity. For  $\gamma > 3(\theta = 3)$ , the distinction between the first regime [Eq. (26)] and the second regime [Eq. (27)] disappears. The particle density decays as  $\rho_s \sim t^{-1}$  for  $t < N^{\bar{z}}$  with  $\bar{z} = 1/2$ , and then saturates to the

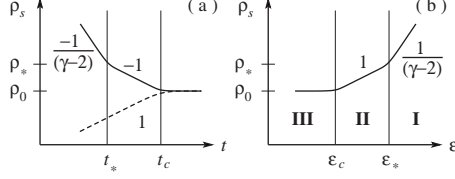


FIG. 1. (a) Schematic plot of  $\rho_s$  vs  $t$  in the log-log scale at the critical point in the annealed networks with  $2 < \gamma < 3$  and  $\omega > \gamma - 1$ . The solid (dashed) line corresponds to the static (defect) dynamics. (b) Schematic plot of  $\rho_s$  vs  $\epsilon$  in the same condition.

stationary-state value  $\rho_s^\infty \sim N^{-1/2}$ . At  $\gamma=3$ ,  $\rho_s \sim (t \log t)^{-1}$  for  $t < t_c \sim (N/\log N)^{1/2}$  and  $\rho_s^\infty \sim (N \log N)^{-1/2}$ .

The systems with the natural cutoff ( $\omega=\gamma-1$ ) are special. Even for  $\gamma < 3$ , the two time scales  $t_*$  and  $t_c$  coincide, having  $\bar{z}_*=\bar{z}=(\gamma-2)/(\gamma-1)$ . This means that the second regime does not exist. The density decays as  $\rho_s \sim t^{-1/(\gamma-2)}$  for  $t < N^{\bar{z}}$ , and then saturates to  $\rho_s^\infty \sim N^{-1/(\gamma-1)}$ . The defect and static dynamics at criticality are illustrated schematically in Fig. 1(a).

### C. Numerical simulations

We have performed numerical simulations in the annealed SF networks to confirm the analytic results. In the defect simulations, the survival probability is expected to scale as

$$\rho_s(t, N) = N^{-\bar{z}\delta} \mathcal{P}(t/N^{\bar{z}}). \quad (31)$$

The scaling function behaves as  $\mathcal{P}(x) \sim x^{-\delta}$  as  $x \rightarrow 0$  and decays exponentially as  $x \rightarrow \infty$ . The particle number averaged over surviving samples is expected to scale as

$$n_s(t, N) = N^{\bar{z}\eta} \mathcal{N}(t/N^{\bar{z}}). \quad (32)$$

The scaling function behaves as  $\mathcal{N}(x) \sim x^{\bar{\eta}}$  as  $x \rightarrow 0$  and converges to a constant as  $x \rightarrow \infty$ .

Figure 2 shows the scaling plots according to the scaling form in Eqs. (31) and (32) with the exponent values in Eqs. (23)–(25). The annealed networks of size  $N=10^3, \dots, 10^6$  were generated with the deterministic method. The plotted data were obtained by averaging over  $10^6$  runs. The nice data

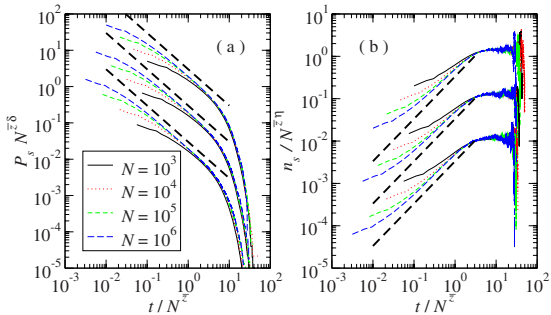


FIG. 2. (Color online) (a) Scaling plot for the survival probability. (b) Scaling plot for the number of particles averaged over surviving samples. The upper, middle, and lower sets of data correspond to the annealed SF networks with  $\gamma=2.5$  and  $\omega=1.5, 2.0$ , and  $3.0$ , respectively. For readability, each data set is scaled down by a constant factor. The dashed lines are guides for the eyes, having slopes of  $-1$  in (a) and  $1$  in (b).

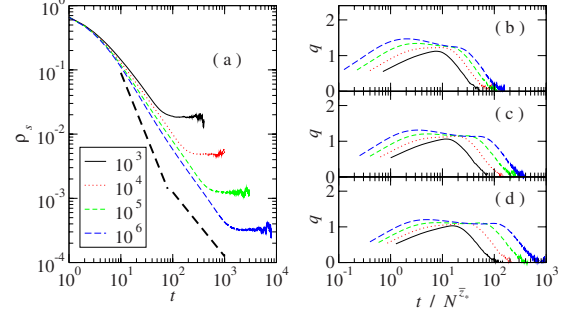


FIG. 3. (Color online) (a) Critical density decay at  $\gamma=2.5$  and  $\omega=2.5$ . The network sizes are  $N=10^3, \dots, 10^6$ . Effective exponent  $q$  versus  $t/N^{\bar{z}*}$  at  $\gamma=2.5$  and (b)  $\omega=2.0$ , (c)  $2.5$ , (d)  $3.0$ .

collapse confirms the validity of the analytic result.

We have also performed the static simulations. Numerical data at the critical point obtained in networks with  $\gamma=2.5$  and  $\omega=2.5$  are presented in Fig. 3(a). Unlike in the schematic plot in Fig. 1, the crossover between two regimes with  $\rho_s \sim t^{-1/(\gamma-2)}$  and  $\rho_s \sim t^{-1}$ , respectively, is not prominent. Moreover, the decay exponents seem to deviate from the expected values significantly. In order to understand the origin of the discrepancy, we have performed a local slope analysis. As an estimate for the density decay exponent, we define an effective exponent  $q(t) \equiv -\ln(\rho_s(t)/\rho_s(t/m))/\ln m$  with a constant  $m=4$ . The effective exponents measured at  $\omega=2.0, 2.5$ , and  $3.0$  are plotted in Figs. 3(b)–3(d), respectively, against the scaling variable  $x=t/N^{\bar{z}*}$ . The analytic theory predicts that  $q$  should converge to  $1/(\gamma-2)=2(1)$  as  $N$  increases for  $x < 1$  ( $x > 1$ ). The effective exponent plot shows a weak but clear tendency toward the analytic prediction. For  $x < 1$ , the effective exponents steadily increase above 1 with network size, but still much lower than the predicted value 2 even for  $N=10^6$ . Moreover there is no appreciable power-law region (flat region for  $q$ ). For  $x > 1$ , the effective exponents overshoot the predicted value 1 until  $N=10^5$ , but start to decrease slightly at  $N=10^6$ . We also notice the appreciable flat region in this case.

In order to identify numerically the power-law scaling in the first regime, it would be required that at least  $t_* \sim 10^2$  (two log decades). With  $\gamma=2.5$  and  $w=2.5$ , the system size must be larger than  $\sim 10^{10}$ , which is beyond the current computer capacity.

We have also studied the FSS behavior of the stationary-state particle density at criticality. It exhibits a power-law scaling with  $N$  as  $\rho_s^\infty \sim N^{-\alpha}$ . It is found (not shown here) that the numerical result for the exponent  $\alpha$  is compatible with the analytic result given in Eq. (30). However, a discrepancy becomes noticeable as  $\gamma$  becomes smaller and  $\omega$  becomes larger due to strong finite-size effects. The degree distribution becomes singular as  $\gamma$  approaches 2. At large  $\omega$ , the maximum degree  $k_{\max} \sim N^{1/\omega}$  grows so slowly that it becomes difficult to observe the asymptotic scaling behavior.

### IV. OFF-CRITICAL SCALING

For  $2 < \gamma < 3$ , the particle density exhibits distinct dynamic characteristics depending on whether  $\rho k_{\max} > 1$  or

$\rho k_{\max} < 1$ . This causes an interesting cutoff-dependent FSS behavior at the critical point. Such a cutoff dependence disappears far from the critical point. However, in finite systems near the critical point, the cutoff dependence can still survive to lead to an anomalous FSS behavior. For  $\gamma > 3$ , the system shows a simple normal FSS behavior.

Near the critical point at  $p=p_c(1-\varepsilon)$ , the rate equation for the density, Eq. (8), reads for  $2 < \gamma < 3$

$$d\rho_s/dt = \varepsilon \rho_s - c' \rho_s^{\gamma-1} \quad \text{for } \rho_s k_{\max} > 1, \quad (33)$$

$$= \varepsilon \rho_s - \frac{1}{2} g \rho_s^2 \quad \text{for } \rho_s k_{\max} < 1, \quad (34)$$

where  $k_{\max} = N^{1/\omega}$ ,  $g = \langle k^2 \rangle / \langle k \rangle^2 \sim N^{(3-\gamma)/\omega}$ , and  $c' = c/2$ .

By setting  $d\rho_s/dt=0$ , one obtains that the stationary-state solution is given by

$$\rho_s^\infty \sim \varepsilon^\beta \quad \text{for } \rho_s k_{\max} > 1, \quad (35)$$

$$\approx 2\varepsilon/g \quad \text{for } \rho_s k_{\max} < 1, \quad (36)$$

with the bulk order-parameter exponent

$$\beta = 1/(\gamma-2). \quad (37)$$

This shows that the stationary-state solution also depends on the degree cutoff  $k_{\max}$ . There is a crossover at  $\varepsilon=\varepsilon_*$  with

$$\varepsilon_* \sim g^{-(\gamma-2)/(3-\gamma)} \sim N^{-1/\bar{\nu}_*} \quad \text{with } 1/\bar{\nu}_* = \frac{\gamma-2}{\omega}. \quad (38)$$

For  $\varepsilon < \varepsilon_*$ , the order-parameter scaling changes into the  $\gamma$ -independent ordinary mean-field linear scaling as in Eq. (36), although this crossover disappears ( $\varepsilon_* \rightarrow 0$ ) in the thermodynamic limit.

When  $\varepsilon$  decreases further below  $\varepsilon_*$ , the system will reach the critical state where the particle density scales as  $\rho_s^\infty \sim \sqrt{1/(gN)}$  [see Eq. (30)]. The critical region in finite systems starts at  $\varepsilon=\varepsilon_c$  with

$$\varepsilon_c \sim \sqrt{\frac{g}{N}} \sim N^{-1/\bar{\nu}} \quad \text{with } 1/\bar{\nu} = \frac{1-(3-\gamma)/\omega}{2}, \quad (39)$$

where the finite-size saturation starts to occur ( $2\varepsilon_c/g = \rho_s^\infty$ ).

The off-critical FSS behavior is illustrated in Fig. 1(b). This scaling theory predicts that there exist two characteristic sizes  $N_* \sim \varepsilon^{-\bar{\nu}_*}$  and  $N_c \sim \varepsilon^{-\bar{\nu}}$  which separate three scaling regimes. In regime I ( $\varepsilon > \varepsilon_*$ ) where  $N_* < N$ , the system behaves as in a SF network with infinite  $N$  and infinite  $k_{\max}$ , e.g.,  $\rho_s \sim \varepsilon^\beta$ . In regime II ( $\varepsilon_c < \varepsilon < \varepsilon_*$ ) where  $N_c < N < N_*$ , it behaves as in a SF network with infinite  $N$  but with finite  $k_{\max}$ . The density scales as  $\rho_s \sim 2\varepsilon/g \sim \varepsilon N^{-(3-\gamma)/\omega}$ . Finally, it behaves as in a SF network with finite  $N$  and  $k_{\max}$  in regime III ( $\varepsilon < \varepsilon_c$ ) where  $N < N_c$ . The density scales as  $\rho_s \sim N^{-\alpha}$  with  $\alpha = (1+(3-\gamma)/\omega)/2$  [see Eq. (30)].

At the special case of the natural cutoff with  $\omega = \gamma - 1$ , regime II disappears and there is a direct crossover from regime I (no size effect) to regime III (critical size scaling). For  $\gamma > 3$  where  $\theta = 3$  and  $g \sim O(1)$ ,  $\rho_s^\infty \sim \varepsilon$  in both regimes I and II, so  $\varepsilon_*$  becomes meaningless. Here again we observe a direct crossover from regime I to regime III.

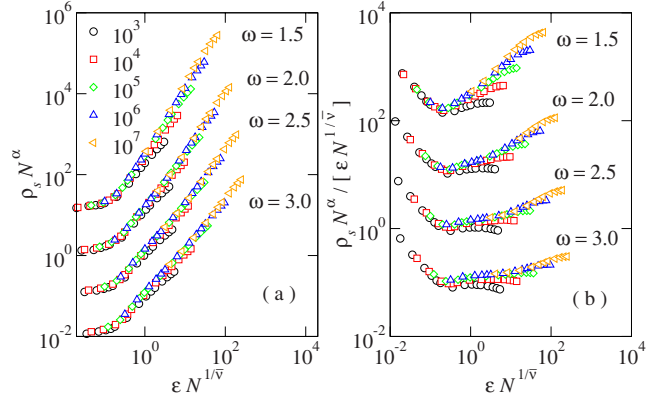


FIG. 4. (Color online) (a) Scaling plots of  $y = \rho_s N^\alpha$  vs  $x = \varepsilon N^{1/\bar{\nu}}$  at  $\gamma = 2.5$  and  $\omega = 1.5, 2.0, 2.5$ , and  $3.0$ . Network sizes are  $N = 10^3, \dots, 10^7$ . (b) Plots of  $y/x$  against  $x$ . Each data set is shifted vertically by a constant factor to avoid an overlap.

The FSS scaling behavior in the annealed SF network is sharply contrasted with that in the quenched SF network. While there are two characteristic sizes  $N_*$  and  $N_c$  that depend explicitly on the degree cutoff in the former (at least for  $2 < \gamma < 3$  and  $\omega > \gamma - 1$ ), it has been proposed in the latter through a droplet-excitation (hyperscaling) argument [4] that there exists a unique cutoff-independent characteristic size  $N_q \sim \varepsilon^{-\bar{\nu}_q}$  with  $1/\bar{\nu}_q = (\gamma-2)/(\gamma-1)$  for  $2 < \gamma < 3$  and  $1/\bar{\nu}_q = 1/2$  for  $\gamma > 3$ . It is interesting to notice that the FSS theory in the annealed network coincides with that in the quenched network for  $\gamma > 3$  and also at the special case with the natural cutoff with  $\omega = \gamma - 1$  for  $2 < \gamma < 3$ . The origin of the discrepancy in the FSS theory between two different networks as well as the relevance/role of the quenched linking disorder have not been fully explored as yet, which awaits a further investigation.

We have performed extensive simulations in the annealed SF networks to test the off-critical FSS theory. In Fig. 4, we present a scaling plot of  $y = \rho_s N^\alpha$  against a scaling variable  $x = \varepsilon N^{1/\bar{\nu}}$  at  $\gamma = 2.5$  and  $\omega = 1.5, 2.0, 2.5$ , and  $3.0$ . When  $\omega = \gamma - 1 = 1.5$  (natural cutoff), the FSS theory predicts that the quantity  $y$  converges to a constant value for  $x \ll 1$  (regime III) and scales as  $y \sim x^{1/(\gamma-2)} = x^2$  for  $x \gg 1$  (regime I). There should be no regime II. The numerical data in Fig. 4 seem to support this two-regime scaling behavior reasonably well.

When  $\omega > \gamma - 1$ , we expect three scaling regimes. The numerical data in regimes II and III will converge to a single curve, but those in regime I should deviate from it because of the two different characteristic sizes. The numerical data in Fig. 4(a) show a clear evidence of regime III (flat region), but a weak signature of regimes II (linear-slope region,  $y \sim x$ ) and I (no collapse). Although the signature is not prominent due to strong finite-size effects, the existence of the three scaling regimes is evident. In Fig. 4(b), we present the numerical data in a different style by plotting  $y/x$  against  $x$ , so regime II can be identified by a flat region. As expected, there is no flat region at  $\omega = 1.5$  (natural cutoff). As  $\omega$  increases, one can see clearly the broadening of the flat region (regime II) which becomes larger with increasing  $N$ . This behavior is qualitatively consistent with the expected FSS behavior. It is very difficult to observe the regime III scaling

even at  $N=10^7$ , similar to the difficulty encountered in the study of the critical dynamics in Sec. III.

Finally, the off-critical dynamic behavior can be easily derived from the rate equations, Eqs. (33) and (34), in the thermodynamic limit, approaching the criticality from the active or the absorbing side,  $\rho_s(t)-\rho_s^\infty \sim e^{-t/\tau}$  where the relaxation time scales as  $\tau \sim \varepsilon^{-\nu_t}$  with  $\nu_t=1$  in all cases. These results are consistent with our previous results through the relaxation-time relations of  $\bar{z}=\nu_t/\bar{\nu}$  and  $\bar{z}_*=\nu_t/\bar{\nu}_*$ .

## V. SAMPLE-TO-SAMPLE FLUCTUATIONS

Suppose that one wants to generate a network of  $N$  nodes with a given degree distribution  $P(k)$  with a (forced or natural) cutoff. In general, there are two kinds of quenched disorder to be considered. First, one should sample a degree sequence  $\{k_1, \dots, k_N\}$  from  $P(k)$  and then choose a way of linking the nodes together to create a network. Disorder can be involved in both processes, which is named as sampling disorder and linking disorder, respectively. A quenched network involves both sampling and linking disorder, in general.

An annealed network is free from the linking disorder. However, it may still have the sampling disorder. In the numerical studies in the preceding sections, we have sampled the degree sequence deterministically without any disorder. On the other hand, probabilistic sampling of the degree sequence leads to the sampling disorder. In this section, we investigate sample-to-sample fluctuations in annealed networks due to the sampling disorder. The quantity of our primary interest is  $g \equiv \langle k^2 \rangle / \langle k \rangle^2$ .

When  $N$  values  $\{k_1, \dots, k_N\}$  are drawn probabilistically in accordance with the distribution  $P(k)$  for  $k_{\min} \leq k \leq k_{\max}$ , a sampled distribution  $\tilde{P}(k) = \sum_{i=1}^N \delta_{k,k_i}/N$  may deviate from the target distribution  $P(k)$  due to the finiteness of  $N$ . The deviation is denoted by  $\delta P(k) = \tilde{P}(k) - P(k)$ . Then, it is straightforward to show that

$$[\delta P(k)] = 0, \quad (40)$$

$$[\delta P(k) \delta P(k')] = -\frac{P(k)P(k')}{N} + \frac{P(k)}{N} \delta_{k,k'}, \quad (41)$$

where  $[\cdots]$  denotes the sample (disorder) average.

The  $n$ th moment of the degree of a sample is given by

$$\langle k^n \rangle \equiv \sum_k k^n \tilde{P}(k) = \langle n \rangle_0 \left( 1 + \frac{\langle n \rangle_\delta}{\langle n \rangle_0} \right), \quad (42)$$

where we introduce shorthand notations as  $\langle n \rangle_0 = \sum_k k^n P(k)$  and  $\langle n \rangle_\delta = \sum_k k^n \delta P(k)$ . There is a  $1/N$  factor in the correlator in Eq. (41). So,  $\langle n \rangle_\delta / \langle n \rangle_0$  can be considered as a small expansion parameter for large  $N$ . Up to the second order, the quantity  $g$  of a given sample can be written as

$$g = \frac{\langle 2 \rangle_0}{\langle 1 \rangle_0^2} \left( 1 + \frac{\langle 2 \rangle_\delta}{\langle 2 \rangle_0} - 2 \frac{\langle 1 \rangle_\delta}{\langle 1 \rangle_0} + 3 \frac{\langle 1 \rangle_\delta^2}{\langle 1 \rangle_0^2} - 2 \frac{\langle 2 \rangle_\delta \langle 1 \rangle_\delta}{\langle 2 \rangle_0 \langle 1 \rangle_0} \right).$$

The disorder-averaged correlators in Eqs. (40) and (41) imply that  $[\langle n \rangle_\delta] = 0$  and that

$$[\langle m \rangle_\delta \langle n \rangle_\delta] = \frac{1}{N} (\langle m+n \rangle_0 - \langle m \rangle_0 \langle n \rangle_0). \quad (43)$$

This allows us to systematically expand  $[g]$  and  $(\Delta g)^2 \equiv [g^2] - [g]^2$  in powers of  $\frac{1}{N}$ . After some algebra, we obtain the following result up to the order of  $1/N$ :

$$[g] = \frac{\langle 2 \rangle_0}{\langle 1 \rangle_0^2} \left\{ 1 + \frac{1}{N} \left( 3 \frac{\langle 2 \rangle_0}{\langle 1 \rangle_0} - 2 \frac{\langle 3 \rangle_0}{\langle 1 \rangle_0 \langle 2 \rangle_0} - 1 \right) \right\} \quad (44)$$

and

$$(\Delta g)^2 = \frac{1}{N} \frac{\langle 2 \rangle_0^2}{\langle 1 \rangle_0^4} \left\{ \frac{\langle 4 \rangle_0}{\langle 2 \rangle_0^2} - 4 \frac{\langle 3 \rangle_0}{\langle 1 \rangle_0 \langle 2 \rangle_0} + 4 \frac{\langle 2 \rangle_0}{\langle 1 \rangle_0^2} - 1 \right\}. \quad (45)$$

Our interest lies in the SF network of  $N$  nodes having the degree distribution  $P(k) \propto k^{-\gamma}$  in the interval  $k_{\min} \leq k \leq k_{\max} = N^{1/\omega}$  with  $\gamma > 2$  and  $\omega \geq \gamma - 1$ . The  $1/N$  term in Eq. (44) is always subleading, so the scaling behavior of  $[g]$  is determined by  $\langle 2 \rangle_0$ , which yields that

$$[g] = \begin{cases} \sim N^{(3-\gamma)/\omega} & \text{for } 2 < \gamma < 3 \\ \sim \log N & \text{for } \gamma = 3 \\ \sim O(1) & \text{for } \gamma > 3. \end{cases} \quad (46)$$

On the other hand, the term  $\langle 4 \rangle_0 / \langle 2 \rangle_0^2$  in the parenthesis of Eq. (45) makes a leading-order contribution. Hence, we find that the relative variance  $R_g = (\Delta g)^2 / [g]^2$  is given by

$$R_g = \begin{cases} \sim N^{(\gamma-1)/\omega-1} & \text{for } 2 < \gamma < 3 \\ \sim N^{2/\omega-1} (\log N)^{-2} & \text{for } \gamma = 3 \\ \sim N^{(5-\gamma)/\omega-1} & \text{for } 3 < \gamma < 5 \\ \sim N^{-1} \log N & \text{for } \gamma = 5 \\ \sim N^{-1} & \text{for } \gamma > 5. \end{cases} \quad (47)$$

In the theory of disordered systems, the relative variance  $R_X$  of an observable  $X$  due to a quenched disorder is an indicator of the self-averaging property [11]. When it vanishes in the thermodynamic limit  $N \rightarrow \infty$ , such a system is said to be *self-averaging*. The self-averaging property implies that an observable measured in a sample with a typical disorder configuration takes the same value as the sample-averaged value in the  $N \rightarrow \infty$  limit. A system with  $R_X \sim N^{-r}$  is said to be *strongly self-averaging* (SSA). This is the case when the central limit theorem works. When  $R_X \sim N^{-r}$  with  $r < 1$ , such a system is said to be *weakly self-averaging* (WSA). A system with strong or relevant disorder lacks the self-averaging property near the criticality. In such a system,  $R_X$  converges to a finite value as  $N$  increases.

The result in Eq. (47) discloses the self-averaging property of the annealed SF network under the sampling disorder. First of all, we find that the system with  $\gamma > 5$  is SSA at all values of the degree cutoff exponent  $\omega$ . For  $\gamma \leq 5$ ,  $R_g$  decays slower than  $N^{-1}$  at all values of  $\omega > \gamma - 1$ . So the system is WSA.

Interestingly, the systems lack the self-averaging property when  $2 < \gamma < 3$  and  $\omega = \gamma - 1$  ( $R_g$  approaches a nonzero constant as  $N$  increases). Note that the cutoff exponent  $\omega = \gamma - 1$  corresponds to the natural cutoff. Networks without explicit constraint on the degree also display the cutoff scaling

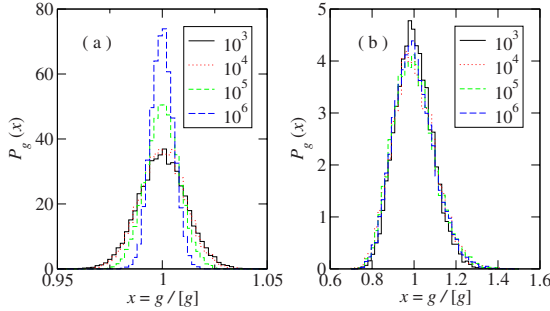


FIG. 5. (Color online) Probability distribution  $P_g(x)$  for  $x=g/[g]$  in the annealed networks with  $N=10^3, \dots, 10^6$ . (a)  $\gamma=2.75$  and  $\omega=3.0$ ; (b)  $\gamma=2.75$  and  $\omega=1.75$ .

$k_{\max} \sim N^{1/(\gamma-1)}$ . In these networks, not only the node-to-node degree fluctuation but also the sample-to-sample degree fluctuations are very strong.

We present the numerical data showing the (non) self-averaging property in Fig. 5. Drawing  $N$  values of  $k$  from the distribution  $P(k) \sim k^{-\gamma}$  in the interval  $2 \leq k \leq N^\omega$ , we calculated  $g = \langle k^2 \rangle / \langle k \rangle^2$ . This was repeated  $N_S = 10^5$  times, from which one can construct the probability distribution function  $P_g(x)$  for  $x = g/[g]$ . Figure 5(a) shows that the distribution becomes sharper and sharper as  $N$  increases. It indicates the self-averaging property at  $\gamma=2.75$  and  $\omega=3.0$ . On the other hand, Fig. 5(b) shows that the distribution converges to a limiting distribution. It indicates that the system is not self-averaging at  $\gamma=2.75$  and  $\omega=\gamma-1=1.75$ .

The strong disorder fluctuation raises an important question. In general, a real complex network is a disordered media having a quenched disorder, for example, the sampling disorder and the linking disorder as mentioned before. Being coupled with dynamic degrees of freedom, the quenched structural disorder may give rise to disorder-relevant critical phenomena. This is a plausible scenario, but has been ignored in most studies. It seems to be a quite challenging problem to incorporate the quenched disorder into a systematic analysis.

In the annealed network considered in this study, the dynamic degrees of freedom are completely decoupled with the sampling disorder (no linking disorder). Hence, the scaling theory developed here should be valid whether the sampling disorder is self-averaging or not. However, our result still warns that the sample average of any observable involving  $g$  is practically meaningless due to its broad distribution, which occurs in the critical region (regimes II and III) in annealed networks with  $2 < \gamma < 3$  and the natural cutoff.

## VI. DISCUSSION AND SUMMARY

We studied the critical behavior of the CP in annealed scale-free networks. For the degree exponent  $\gamma > 3$ , the standard single-parameter FSS is found with various dynamic and static exponents which are independent of the cutoff exponent  $\omega$  and also  $\gamma$ . For highly heterogeneous networks with  $\gamma < 3$ , there exist two different characteristic time scales and their associated exponents depend not only on  $\gamma$  but also on  $\omega$ . These results are contrasted with those in the quenched scale-free networks where a single-parameter FSS is found without any cutoff dependence even for  $\gamma < 3$  if the cutoff is not strong enough ( $\omega < \gamma$ ) [4,12]. At the special case of  $\omega = \gamma - 1$  (natural cutoff), these two different FSS coincide to each other.

Annealed networks may include the sampling disorder, which generates a strong sample-to-sample fluctuation in highly heterogeneous networks with the natural cutoff. In quenched networks, the linking disorder is inherent, which generates the density-density correlation in neighboring nodes through coupling with fluctuating variables. This correlation leads to the shift of the transition point of the CP model [12,13]. In addition, the linking disorder generates another type of sample-to-sample fluctuations which cause spreading of the transition points in finite systems. Hong *et al.* [4] showed that there exists a characteristic (droplet) size scale diverging as  $N_q \sim \varepsilon^{-\bar{\nu}_q}$  with  $1/\bar{\nu}_q = (\gamma-2)/(\gamma-1)$  for  $\gamma < 3$ . For  $N < N_q$  (or equivalently  $\varepsilon < \varepsilon_q$  with  $\varepsilon_q \sim N^{-(\gamma-2)/(\gamma-1)}$ ), the system feels the droplet length scale and the finite-size effect is dominant. As  $\varepsilon_q > \varepsilon_c$  given in Eq. (39), one may expect that the finite-size saturation induced by the droplet length scale comes in earlier (at  $\varepsilon = \varepsilon_q$ ) in quenched networks than in annealed networks. Then, the cutoff dependency of the saturation density may disappear. However, as  $\varepsilon_q < \varepsilon_*$  given in Eq. (38), the cutoff-dependent density-decaying dynamics comes in before saturation. The linking disorder fluctuation may be responsible for the disappearance of this dynamics in the quenched networks, but this is just a speculation as yet. A full understanding of the FSS behavior in quenched networks needs a further investigation.

*Note added.* Recently, Boguñá *et al.* posted a preprint [14]; the results of which partially overlap with those presented here.

## ACKNOWLEDGMENTS

This work was supported by KOSEF grant Acceleration Research (CNRC) (Grant No. R17-2007-073-01001-0). This work was also supported by the Korea Research Foundation grant funded by MEST (Grant No. KRF-2006-003-C00122).

- 
- [1] S. N. Dorogovtsev, A. V. Goltsev, and J. F. F. Mendes, Rev. Mod. Phys. **80**, 1275 (2008).
  - [2] D. J. Watts and S. H. Strogatz, Nature (London) **393**, 440 (1998).
  - [3] A.-L. Barabási and R. Albert, Science **286**, 509 (1999).
  - [4] H. Hong, M. Ha, and H. Park, Phys. Rev. Lett. **98**, 258701 (2007).
  - [5] C. Castellano and R. Pastor-Satorras, Phys. Rev. Lett. **100**,

- 148701 (2008).
- [6] H. Hinrichsen, Adv. Phys. **49**, 815 (2000).
- [7] K.-I. Goh, B. Kahng, and D. Kim, Phys. Rev. Lett. **87**, 278701 (2001).
- [8] M. Catanzaro, M. Boguñá, and R. Pastor-Satorras, Phys. Rev. E **71**, 027103 (2005).
- [9] W. M. Hwang, S. Kwon, H. Park, and H. Park, Phys. Rev. E **57**, 6438 (1998).
- [10] M. E. Fisher, J. Stat. Phys. **34**, 667 (1984).
- [11] A. Aharony and A. B. Harris, Phys. Rev. Lett. **77**, 3700 (1996).
- [12] M. Ha, H. Hong, and H. Park, Phys. Rev. Lett. **98**, 029801 (2007).
- [13] C. Castellano and R. Pastor-Satorras, Phys. Rev. Lett. **96**, 038701 (2006).
- [14] M. Boguñá, C. Castellano, and R. Pastor-Satorras, Phys. Rev. E **79**, 036110 (2009).